Enhanced Rolling Moment of Inertia Demonstration

Jerome C. Licini, Richard O. White, George Awad, and Yoon Jung Choi

Physics Department, Lehigh University, Bethlehem, PA 18015

(Dated January 10, 2023)

Abstract

Moment of inertia is often illustrated using the classic demonstration of a solid cylinder and a hollow cylinder with identical mass and radius rolling down an incline, in which the solid cylinder has a linear acceleration $4/3$ times that of the hollow cylinder. This article describes an extreme version of this apparatus with a rolling object that has an acceleration more than 25 times that of an object of identical mass and rolling radius. This apparatus would be suitable as a lecture demonstration or as an intermediate-level laboratory project.

I. INTRODUCTION

A classic lecture demonstration to illustrate the effect of moment of inertia is to compare a hollow and a solid cylinder rolling down a ramp.[1] The two cylinders have the same mass and radius, but the solid one has a greater acceleration by a factor of $4/3$ due to the different distribution of the mass (as expressed analytically via moment of inertia). This paper describes an extreme version of the classic demonstration that shows a difference in acceleration by more than a factor of 25 between two objects. Our objects each have a thin axle that rolls down the ramp, but they have end pieces that overhang the edges of the ramp, allowing for a greater variation in moment of inertia.

The need for demonstrations on this topic is important and ongoing. The classic 1938 book on physics demonstrations by Sutton[2] describes several clever rolling devices that can be used to qualitatively illustrate the effect of moment of inertia but does not focus on the comparison and quantitative aspects that have made the hollow and solid cylinder demonstration so ubiquitous. A 2018 paper by Hazlett and Aragoneses describes a 3D-printed wheel that allows students to quantitatively vary its moment of inertia while keeping mass and radius constant, but they present results that focus on its use in Atwood machine configurations.[3] The crux of our demonstration is separating the radius of the rolling component from the exterior dimensions of the object, which is a phenomenon that is also exploited in a 2006 paper by Niculescu which achieves a 25% variation of acceleration by rolling a solid sphere down U-shaped channels with varying widths, but the moment of inertia itself is not varied.[4] Very recent examples of the continuing interest in this rolling demonstration can be found for cylinders containing liquid in papers in 1996 by Jackson et al.,[5] in 2015 by Lin et al.[6] and in 2020 by Greenslade.[7] As Lin et al. point out, "The analysis of the dynamics of the bodies sliding and rolling on a ramp is a standard component of

introductory physics classes, and a required component of the Advanced Placement (AP) Physics curriculum."

II. ROLLING CALCULATIONS

The comprehensive analysis of rolling motion requires subtleties of interpretation that are difficult to treat at the introductory level. A recent review of the classic hollow and solid cylinder demonstration was presented by Phommarach *et al*.[8] In their paper, they clearly explain the role of friction in determining the allowable angles for rolling without slipping and demonstrate the techniques required for video analysis of rolling cylinders. Rimoldini and Singh[9] investigate student understanding of rolling concepts and suggest instructional strategies. Carnero *et al.*[10] propose a framework for presenting the difficult issue of the role of friction in rolling.

In order to focus on the moment of inertia contribution, however, we merely outline the simplest case for "rolling without slipping." In an energy analysis, the motion of the rolling object is treated as the combination of the translational velocity v of the center of mass and the rotational velocity ω of the object around that center of mass. The kinetic energy of a rolling object is then given as $K = \frac{1}{2}Mv^2 + \frac{1}{2}I\omega^2$. Rolling without slipping requires a relationship of $v = \omega r$ where r is the radius of contact between the rolling object and the surface. This yields $K = \frac{1}{2}Mv^2 + \frac{1}{2}I(v/r)^2 = [1 + (I/Mr^2)]\frac{1}{2}Mv^2$. We will define $C \equiv [1 + (I/Mr^2)]$ since this factor will facilitate comparisons between objects with different mass distributions. If the object was released from rest at an initial position which is a vertical distance $h = s\,sin\theta$ above the final position, where s is the length of the ramp and θ is its angle relative to horizontal, then the potential energy at that initial position is given as $U_i = Mgh = Mgs\,sin\theta$. Neglecting any non-conservative forces yields $K_f = U_i$ and reveals the final velocity of the object to be

$$v_f = \sqrt{2\ g\ s\ sin\ \theta / C} \qquad (1)$$

Expressions for the time taken for the rolling object to travel a distance *s* after starting from rest and the linear acceleration can then be obtained as follows:

$$t = \frac{s}{v_{average}} = \frac{s}{(0+v_f)/2} = \frac{2s}{v_f} = \sqrt{\frac{2sC}{g\ sin\ \theta}} \qquad (2)$$

$$a = \frac{v_f}{t} = \frac{g\ sin\ \theta}{C} \qquad (3)$$

In all of these equations, the factor *C* encapsulates the differences between rolling objects. For example, to model an object that has no rotational contribution to its kinetic energy, *I*=0, *C*=1, and we obtain the familiar results of $a = g\ sin\ \theta$, $v_f = \sqrt{2\ g\ s\ sin\ \theta}$, and $t = \sqrt{\frac{2s}{g\ sin\ \theta}}$ for an object sliding down a frictionless ramp.

For the classic demonstration with hollow and solid cylinders, the rolling radius *r* is simply equal to the geometric radius *R* of the cylinder. An ideal hollow cylinder has $I = 1MR^2$ and *C*=2 while a solid cylinder has $I = \frac{1}{2}MR^2$ and $C = \frac{3}{2}$, so the *C* factors have a relative ratio of $\left(2/\frac{3}{2}\right) = \frac{4}{3}$. Therefore, relative to the hollow cylinder, the solid cylinder has $4/3 = 1.33$ times the acceleration, $\sqrt{4/3} = 1.15$ times the final velocity, $\sqrt{3/4} = 0.866$ times the time of descent.

III. ENHANCED ROLLING INERTIA APPARATUS

In order to present a more striking difference than that provided by the hollow and solid cylinders, we developed objects which roll down a ramp on a small-diameter shaft which has a length greater than the width of the ramp. Since the ends overhang the ramp, we can produce a

wider variation in moments of inertia while still maintaining the same total mass and rolling radius in analogy with the solid and hollow cylinder demonstration.

Prototypes were first built using electrical conduit for the axles, but these had problems with straightness and uniformity, so in order to make the second generation objects more precisely symmetrical, higher quality aluminum tubing was used for the axles.[11] The high moment of inertia object used end pieces which were 14-inch diameter plastic wheels designed for garden carts.[12] Two adapters were machined to fix the wheels to the ends of the aluminum tubing so they could not rotate relative to the aluminum tubing. The low moment of inertia object used end pieces which were 4-inch diameter solid steel cylinders with the center bored out to slide over the tube and secured with side set screws. The lengths of the tubes and the steel cylinders were fabricated so that the two assemblies had the same total length of 137 ± 1 cm and the same total mass of 3.30 ± 0.01 kg. Since these end pieces have very different radii, they clearly have very different moments of inertia. See upper photo of Figure 1.

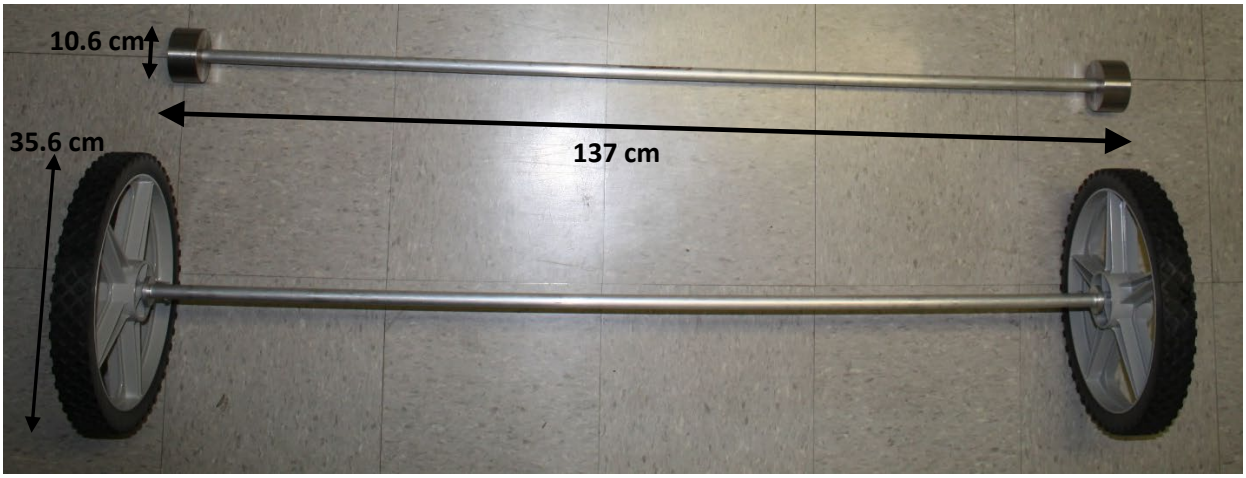

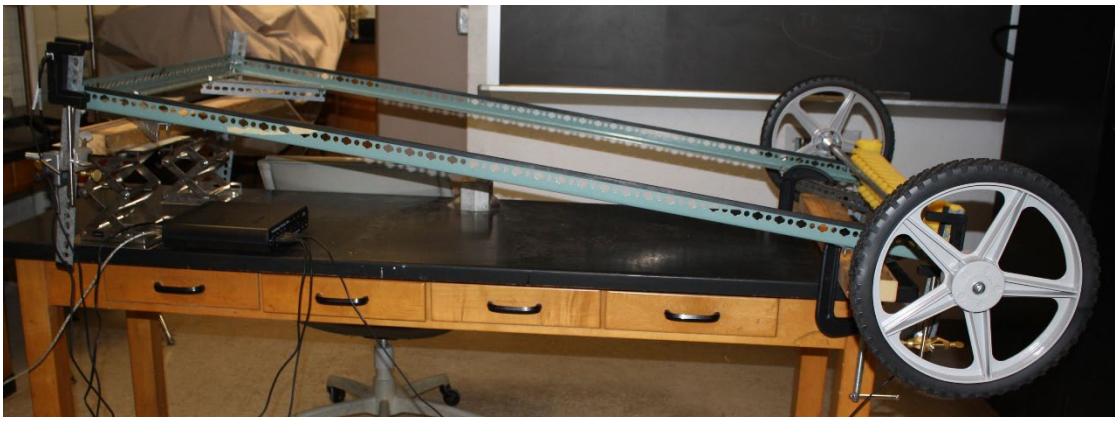

FIG. 1. The upper photograph shows objects for the rolling moment of inertia demonstration. As opposed to the traditional lecture demonstration which uses a hollow and solid cylinder that have an acceleration ratio of 1.33, the objects shown have equal mass and rolling radius, but an acceleration ratio of more than 25. The lower photograph shows the ramp with photogates.

Due to its complex shape, we determined the moment of inertia of the plastic wheel empirically, using the rotational dynamics student experiment in our introductory mechanics laboratory course. For consistency, we measured the steel ends in the same way. The student experiment consists of a PASCO Rotating Platform (model ME-8951), a Rotational Inertia Accessory (ME-8953), a Photogate Head (ME-9498A), a PASCO 550 Universal Interface (UI-5001), and PASCO Capstone software. This experiment measures the angular acceleration α of a rotating object with moment of inertia I due to a string that wraps around its shaft of radius r with the other end of the string attached to a hanging mass m. The presence of a frictional torque τ_f produces a negative angular acceleration of α' with no hanging mass. (Each configuration was repeated for four runs to find an average value of the angular acceleration.) Newton's Law for the angular motion then yields $\tau_{net} = mgr - \tau_f = (I + mr^2)\alpha$. In practice, both the moment

of inertia contribution of the hanging mass and the frictional torque yield corrections of less than 1%. Nevertheless, for the sake of physics modeling, we manipulate the above equation to yield $\left[\frac{\alpha-\alpha'}{gr-r^2\alpha}\right] = \frac{m}{I}$. We therefore plotted the fraction on the left side versus four different but equally spaced values of the hanging mass *m* to do a linear fit which yields a slope equal to the inverse of the moment of inertia of the rotating object, (1/*I*). Three rotating object configurations were measured: the PASCO disk itself, the disk plus the two steel endcaps, and the disk plus the two plastic wheels.

In contrast, the aluminum tube cannot be measured with the PASCO apparatus, so we calculate its moment of inertia by using the formula for an annulus with uniform density, $\frac{1}{2}M({r_2}^2 + {r_1}^2)$. Measurements of the aluminum tube described an annulus of mass 0.562 ± 0.001 kg with an outer radius of 0.95 ± 0.013 cm and an inner radius of 0.64 ± 0. 013 cm for an expected moment of inertia of 0.366 ± 0.006 kg cm^2. This aluminum tube will be a small contribution compared to the steel ends or plastic wheels.

The experimental value obtained for the combined moment of inertia of the pair of steel ends was 20.9 ± 1.1 kg cm^2. This is in good agreement with the theoretical value of 21.1 kg cm^2 for a pair of objects where each is an annulus with mass 1.37 kg, with an inner radius of 0.96 cm and an outer radius of 3.81 cm. After adding the calculated value for the aluminum tube, the apparatus with the aluminum tube and two steel end pieces has a moment of inertia of 21.2 ± 1.1 kg cm^2. The value obtained for the pair of plastic wheels was 581.0 ± 2.0 kg cm^2. Since each plastic wheel has a mass of 1.33 kg and an outer radius of 17.8 cm, this measured moment of inertia represents a reasonable value of 0.69 times its MR^2, which for a wheel with spokes is appropriately intermediate between the theoretical values of ½ for a solid disk and 1 for

a hollow rim. After adding the calculated value for the aluminum tube, the apparatus with the aluminum tube and two plastic wheels has a moment of inertia of 581.4 ± 2.0 kg cm^2.

Despite their very different overall radius, both of our objects have the same mass of 3.30 ± 0.01 kg, and the same value of the rolling radius of their axle, r = 0.95 ± 0.013 cm. The factor of $C \equiv [1 + (I/Mr^2)]$ can be at most 2.0 for an object that rolls on its outer radius, but for these objects with a deliberately small rolling radius, C can become much larger. For the apparatus with the steel end pieces, C is 8.13 ± 0.66, while for the object with the plastic wheels, C is 196.2 ± 6.7, so the C factors have a relative ratio of 24.1 ± 2.8. Therefore, relative to the object with the plastic garden tractor wheels, the object with the steel end pieces therefore is predicted to have 24.1 ± 2.8 times the acceleration, $\sqrt{24.1 \pm 2.8} = 4.91 \pm 0.28$ times the final velocity, and $\sqrt{1/(24.1 \pm 2.8)} = 0.204 \pm 0.012$ times the time of descent.

IV. EXPERIMENTAL RESULTS

The new rolling objects were placed on a rectangular frame 1.6 m long by 0.77 m wide made from Steelworks 6-ft x 2-1/4-in Plated Steel Slotted Angle (requiring 3 pieces at $23 each). In order to increase the coefficient of friction between the aluminum tube and the rectangular frame, rubber trim pieces were applied to the two top edges of the rectangular frame.[13] One end of this frame was raised with lab jacks to provide a vertical drop of 24.0 ± 0.5 cm for a ramp angle of 8.5 ± 0.2° above horizontal. Timing information was obtained using three PASCO photogates, one just below the starting position at the top of the frame, a second photogate a distance 0.82 ± 0.02 cm from the first one, and a third photogate just above the bottom of the frame, with a distance of 149.4 ± 0.5 cm from the first one. The photogates were connected to a PASCO Science Workshop 750 Interface USB data acquisition module connected to a Windows

personal computer. The PASCO Capstone software suite and Excel spreadsheets were used to record and analyze the data.[14] Each object was rolled down the incline 10 times and the linear accelerations were calculated using the three-photogate method of Venable, *et al*.[15] The average values of acceleration obtained were 14.57 ± 0.27 cm/s^2 for the object with the steel endpieces and 0.564 ± 0.025 cm/s^2 for the object with the garden tractor wheels. Compared with the 33.3% difference available with the traditional rolling cylinders, this demonstration shows a more than 2,500% larger acceleration of the assembly with the lower moment of inertia. The 25.8 ± 1.6 times larger acceleration observed is in agreement with the 24.1 ± 2.8 times larger acceleration predicted above.

In lecture, it is instructive to do the hollow and solid cylinder demonstration first, especially since this is the configuration analyzed in their textbook and the lecture. Although the difference in travel times between the two cylinders is only 14%, by releasing the two cylinders at the same time, students can easily hear two separate impacts and see that the solid cylinder reaches the bottom of the ramp before the hollow cylinder. With that freshly in mind, we follow with the new demonstration, starting with the steel endcap object and timing its travel down the incline by hand using a stopwatch. (The photogate measurements yielded 4.50 ± 0.06 s.) Then the plastic wheel object was placed at the top of the incline and a serious show was made of preparing to time the descent with the stopwatch. Moments after release, however, it became obvious to the students that a stopwatch was not needed to demonstrate the drastic difference in descent time between the two objects. (The photogate measurements yielded 22.8 ± 0.7 s.) This result was further reinforced by restarting the steel cylinder from rest below the already rolling plastic wheel object to vividly demonstrate how much faster it accelerates and still reaches the

bottom of the ramp before the plastic wheel object. As a consistency check, the 5.07 ± 0.22 ratio of these experimental times agrees with the 4.91 ± 0.28 ratio of the times predicted above.

Please note that a video of this demonstration is available online.[16]

V. ACKNOWLEDGEMENTS

We would like to acknowledge the excellent fabrication and design assistance provided by John Gregoris. We also acknowledge helpful conversations with Jeffrey Stephens, Kebra Ward, and Dave Slimmer.

---

[1] J. Solbes and F. Tarín, "Which Reaches the Bottom First?" Phys. Teach., 46, 550-551 (2008). Also see for example Example 10.5 in H. D. Young and R. A. Freedman, *University Physics*, 14th edition (Pearson Education, 2016) p. 312.

[2] R. M. Sutton, *Demonstration experiments in physics*, 1st edition (AAPT, McGraw-Hill, 1938) p. 69.

[3] E. Hazlett and A. Aragoneses, "A 3D-Printed Wheel with Constant Mass and Variable Moment of Inertia for Lab and Demonstration," Phys. Teach., **56** (8), 535-537 (2018).

[4] A. Niculescu, "A Rolling Sphere Experiment," Phys. Teach., **44** (2), 157-159 (2006).

[5] K. A. Jackson et al, "Viscous and nonviscous models of the partially filled rolling can," Am. J. Phys. 64, 277-282 (1996);

[6] S. Lin et al., "Simple Model of a Rolling Water-Filled Bottle on an Inclined Ramp," Phys. Teach. 53, 548 (2015).

[7] T. B. Greenslade, "Rolling Soup Cans Down an Inclined Plane," Phys. Teach. 58, 387 (2020).

[8] S. Phommarach, P. Wattanakasiwich, and I. Johnston, "Video analysis of rolling cylinders," Phys. Educ. **47** (2), 189-196 (2012).

[9] L. G. Rimoldini and C. Singh, "Student understanding of rotational and rolling motion concepts," Phys. Rev. Spec. Topics – Phys. Educ. Res. **1**, 010102 (2005).

[10] C. Carnero, J. Aguiar, and J. Hierrezuelo, "The work of the frictional force in rolling motion," Phys. Educ. **28** (4), 225-227 (1993).

[11] 6061 Aluminum Round Tube, 3/4" outer diameter, 1/8" wall thickness, 6 ft. long, purchased from McMaster-Carr, Stock #9056K33.

[12] Arnold 14-inch diameter Plastic Wheel, SKU: 006740450, $17 each, Arnolds Lawn Care, Huntsville, Texas. www.arnoldparts.com and many vendors.

[13] Neoprene Rubber U-Channel Push-on Trim, 1/16" Wide x 1/4" High Inside (requiring two pieces 10 ft long, McMaster-Carr #8507K52 at $9 each).

[14] Michael Paskowitz at PASCO provided a Capstone workbook for three-photogate data logging.

[15] D. D. Venable, A. P. Batra, and T. Hubsch, Phys. Teach., **39** (4), 215-217 (2001).

[16] <https://www.lehigh.edu/~jcl3/ExtremeVersion-RollingInertia> or <https://drive.google.com/file/d/1T9a_AeNcktwc4ZkU24_sMuNs3lgUTnR_/view?usp=sharing>

TABLE I. Summary of measured and calculated kinematic quantities for the object with the steel end pieces and the object with the plastic wheel end pieces, and their ratios. These ratios are significantly enhanced relative to those for the traditional solid and hollow cylinder demonstration (theoretical ratios shown in bottom line).

	Final velocity (cm/s)	Time (s)	Linear acceleration (cm/s^2)
Steel ends	65.6 ± 1.5	4.50 ± 0.06	14.57 ± 0.27
Plastic wheel ends	12.8 ± 0.7	22.8 ± 0.7	0.564 ± 0.025
Ratio for this demonstration (steel/wheel)	5.10 ± 0.30	0.197 ± 0.007	25.8 ± 1.2
Ratio for traditional demonstration (solid/hollow cyl)	1.15	0.866	1.33